Journal of Molecular Liquids 314 (2020) 113639

Contents lists available at ScienceDirect

Journal of Molecular Liquids

journal homepage: www.elsevier.com/locate/molliq

Insights into the interaction between lipid bilayers and trehalose aqueous solutions

Amit Kumar [a], Alberto Cincotti [b], Santiago Aparicio [c,d,*]

[a] Department of Electrical and Electronic Engineering, University of Cagliari, 09123 Cagliari, Italy
[b] Department of Mechanical, Chemical and Materials Engineering, University of Cagliari, 09123 Cagliari, Italy
[c] Department of Chemistry, University of Burgos, 09001 Burgos, Spain
[d] International Research Center in Critical Raw Materials for Advanced Industrial Technologies (ICCRAM), University of Burgos, 09001 Burgos, Spain

ARTICLE INFO

Article history:
Received 20 March 2020
Received in revised form 15 June 2020
Accepted 17 June 2020
Available online 20 June 2020

Keywords:
Anhydrobiosis
Dry preservation
Trehalose
Water solutions
Lipid membranes
Molecular dynamics

ABSTRACT

The properties of lipid bilayers in contact with trehalose solutions in water were studied in the full concentration range using molecular dynamics simulations. The mechanism of trehalose interaction with the bilayer surface was analysed considering hydrogen bonding and molecular arrangements as well as the possible changes in bilayer properties. The effect of concentration of the possible mechanisms of trehalose action as membrane protectant were discussed to infer the possible evolution of water replacement by trehalose at the membrane surface and its relationship with the trehalose role in anhydrobiosis and drying processes.

1. Introduction

The living organisms have developed numerous strategies for survival under extreme conditions among which cryptobiosis [1], i.e. metabolic activity reduced to undetectable levels, is particularly relevant. A well-known, and particularly relevant mechanism for cryptobiosis is anhydrobiosis [2], in which organism can survive under almost totally anhydrous conditions. Likewise, the preservation of biological materials for practical purposes requires to develop drying procedures and cryopreservation methods [3], for which the action of cryoprotective solutes needs to be properly understood using information from anhydrobiosis processes developed in nature.

Anhydrobiosis is characterized by the accumulation of large amounts of saccharides [4] in the cell, in particular of trehalose dissacharide (THAL, Fig. 1) [5,6]. Saccharides can develop bio protection both for the stabilization of biomolecules [7] as well as for lipid membranes [8–10]. In the case of cell membranes, the protecting role of saccharides stands on the elimination of lipid phase transitions [11,12], to a gel-like phase, which may modify the membranes cell transports. There are two main hypothesis on the possible mechanism(s) in which saccharides as THAL are able to avoid these lipid bilayer phase transitions: i) the so-called water replacement hypothesis (WRH) [13,14], which considers that during drying saccharides replace water molecules in the hydrogen bonding with polar headgroups in the lipid chains, and ii) the hydration forces hypothesis (HFH) [15], which considers that sugar molecules are excluded from the membrane surface, thus reducing compressive stress as membranes comes together upon drying, which hinders lipid bilayers phase transition. Additional mechanisms have been proposed [16] as the headgroup bridging hypothesis, the vitrification hypothesis and water entrapment hypothesis. The available experimental literature has showed some evidences for all these hypotheses [17], and even it has been suggested that some of these hypothesis may be complementary and not necessarily exclusive [16]. Therefore, there is controversy, despite the large number of available studies, for the role(s) of saccharides as THAL acting on bilayers with two main possible acting mechanisms, i.e. THAL interacting with membranes surfaces or being excluded from the surface.

The clarification of THAL–bilayers interactions has been approached both by experimental and molecular modelling studies. In particular classical molecular dynamics simulations (MD) have proved to be useful for inferring nanoscopic level details including THAL interaction with model lipid bilayers as well as changes in the membrane properties and structuring in presence of THAL molecules, which can be used for providing validation of the available hypotheses of THAL protection action upon drying. Villareal et al. [18] carried out MD studies of 1,2-dipalmitoyl-sn-glycero-3-phosphocholine (POPC) bilayer interacting with THAL, thus suggesting the formation of long-lived hydrogen

* Corresponding author.
E-mail address: sapar@ubu.es (S. Aparicio).

https://doi.org/10.1016/j.molliq.2020.113639
0167-7322/

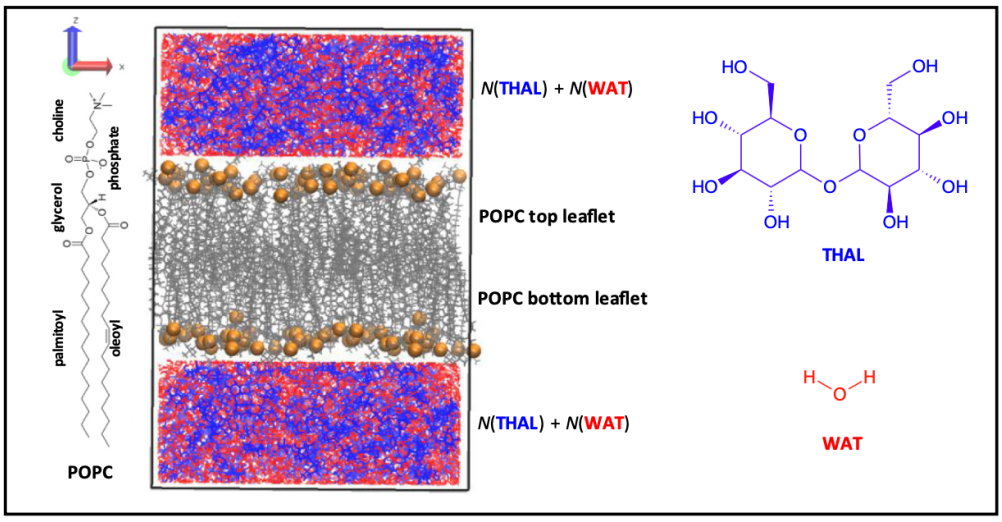

Fig. 1. Scheme of systems used in this work for MD simulations of THAL + WAT mixtures on top and below POPC leaflets in POPC bilayers. Orange spheres show P atoms in POPC molecules, which are used to define bilayer thickness.

bonding between THAL and lipid headgroups but maintaining the features of lipid membranes in terms of lipid area or lipid order parameters. Pereira et al. [19] studied dipalmitoylphosphatidylcholine (DPPC) bilayers interacting with THAL by MD and showed hydrogen bonding with lipids headgroups but without total replacement of water molecules on the bilayer surface, thus pointing to WRH but without being able to discard other cooperative mechanisms. DPPC–THAL systems were also studied by Skibinsky et al. [20] at high hydration states providing proofs of WRH. Horta et al. [16] studied THAL, as well as gentobiose dissacharide, interacting with DPPC bilayers, with their MD results being compatible with four different action mechanisms, including WRH, thus suggesting that multiple mechanisms may be responsible of THAL protective function as well as rising the need of an accurate definition of the possible mechanisms of action to be validated both experimentally and theoretically. Kapla et al. [21] carried out MD simulations of a 1,2-dimyristoylsn-glycero-3-phosphocholine (DMPC) bilayer plus THAL systems providing proofs for the WRH. Liu et al. [22] used MD to study POPC–THAL systems under mechanical stress showing the prevailing role of water replacement effect.

Therefore, the available MD, and experimental, literature on THAL–bilayers interactions still lacks conclusive proofs for THAL mechanism of action. Andersen et al. [23] proposed reconciliation views of THAL interactions or exclusion considering that for low THAL concentration (i.e. initial stages of drying) THAL molecules are accumulated at the interface in contrast with high THAL concentrations (i.e. final stages of drying) for which THAL molecules are expelled from the surface, thus providing the relevant role of THAL concentration and the possible development of different mechanisms along the different stages of drying processes. On the contrary, Kent et al. [17] showed that THAL molecules do not strongly associates with membranes, discarding direct THAL–surface interactions as the mechanisms of protective action for THAL molecules. Hence, there is a clear need to clarify and discard ambiguities for THAL mechanism(s) of action regarding bilayers, showing THAL concentration effect in the whole range for drying purposes because anhydrobiosis is still an unsolved problem [24]. In this work, we report a detailed MD study on THAL–POPC bilayers interactions covering from low concentration THAL solutions to neat THAL to study structural and intermolecular forces along the whole drying process. The reported results allowed delving the mechanism of THAL action during drying procedures by analysing the available hypotheses as a function of dehydration evolution.

2. Methods

All atoms MD simulations for THAL–WATER–POPC bilayers were carried out using ACEMD [25] software. POPC lipid was selected for modelling cell membranes as it is naturally present in eukaryotic cells [26] and it has been previously used for modelling THAL behaviour and mimicking cell membranes [27]. A lipid bilayer consisting in 83 + 83 POPC molecules (for upper and lower leaflet contents) was built using CHARM-GUI builder [28], thus leading to 70 × 70 Å^2 surface area per leaflet. A liquid layer containing THAL + water at the different concentrations (Table 1) was placed on top of each leaflet, thus corresponding to different water content in contact with the bilayer. A simulation containing pure THAL was considered as reference, and, although it is an unphysical system, it is used as a limit situation to be compared with the remaining water + THAL solutions considered in Table 1 to study different stages of dehydration. It should be remarked that each bilayer leaflet is placed in contact with the reported number of THAL and WATER molecules, Fig. 1. The initial simulation boxes, Fig. 1, were built with PACKMOL software [29]. CHARMM36 forcefield was used for POPC molecules [30,31], water molecules were described using TIP3P model [32,33], and THAL molecules were described using CHARMM general force field (CGenFF) [34]. The description of THAL–POPC systems by using CHARMM FF have proven to be reliable in previous studies [27]. Lennard-Jones non-bonded cross terms were

Table 1
Systems used for MD simulations along this work. *N* stands for the number of molecules, x_{THAL} for THAL mole fraction, and wt% (THAL) for THAL mass percentage in the solution in contact with the corresponding lipid bilayer. Values are reported per lipid bilayer leaflet, i.e. each leaflet contains the reported number of POPC molecules and is placed in contact with the reported number of THAL and WATER molecules, Fig. 1.

Label	*N*(THAL)	*N*(WAT)	*N*(POPC)	x_{THAL}	wt% (THAL)
WAT	0	12,500	83	0	0
S_01	50	12,500	83	0.0040	7.1
S_02	100	11,000	83	0.0090	14.7
S_03	150	9500	83	0.0155	23.1
S_04	200	8000	83	0.0244	32.2
S_05	250	6500	83	0.0370	42.2
S_06	300	5000	83	0.0566	53.3
S_07	330	4100	83	0.0745	60.5
THAL	455	0	83	1	100

Table 2
Properties of systems obtained from MD simulations for the last 100 ns of the simulations (1000 ns total simulation time). A_{POPC} stands for the area per lipid; h stands for the thickness of the POPC bilayer; D_L stands for the POPC lateral diffusion (xy plane in Fig. 1); ω_ρ stands for the width of the interdigitation region between upper and lower leaflets; Θ_{PN}, $\Theta_{sn\text{-}1}$ and $\Theta_{sn\text{-}2}$ stands for the angle formed between PN, sn-1 and sn-2 vectors (defined in Fig. S1, ESI) and bilayer normal (z-axis). All values at 303 K and 1 bar. Standard deviations for each property are reported.

System	A_{POPC}/nm^2	h/nm	$10^8\ D_L$/cm^2 s^{-1}	ω_ρ/nm	Θ_{PN}/deg	$\Theta_{sn\text{-}1}$/deg	$\Theta_{sn\text{-}2}$/deg
WAT	0.644 ± 0.017	3.940 ± 0.196	13.0 ± 0.4	0.464 ± 0.044	74.3 ± 1.9	148.5 ± 1.5	146.3 ± 1.6
S_01	0.688 ± 0.020	3.797 ± 0.158	2.039 ± 0.116	0.567 ± 0.023	66.5 ± 2.1	144.9 ± 1.6	146.2 ± 1.6
S_02	0.684 ± 0.020	3.793 ± 0.130	1.552 ± 0.052	0.543 ± 0.026	65.5 ± 2.0	144.5 ± 1.6	145.4 ± 1.5
S_03	0.680 ± 0.070	3.838 ± 0.155	0.897 ± 0.048	0.635 ± 0.026	67.4 ± 2.0	146.0 ± 1.6	147.4 ± 1.4
S_04	0.676 ± 0.066	3.832 ± 0.134	0.444 ± 0.051	0.530 ± 0.035	69.5 ± 2.1	145.1 ± 1.5	145.2 ± 1.7
S_05	0.678 ± 0.075	3.754 ± 0.130	0.228 ± 0.062	0.630 ± 0.041	72.1 ± 2.5	144.2 ± 1.9	145.3 ± 1.8
S_06	0.670 ± 0.060	3.696 ± 0.131	0.177 ± 0.055	0.655 ± 0.027	78.5 ± 1.9	145.8 ± 1.8	148.0 ± 1.5
S_07	0.669 ± 0.057	3.625 ± 0.103	0.081 ± 0.030	0.779 ± 0.024	82.8 ± 1.8	144.6 ± 1.8	143.5 ± 1.8
THAL	0.688 ± 0.071	3.531 ± 0.127	0.004 ± 0.001	0.790 ± 0.026	83.3 ± 2.0	133.7 ± 2.2	136.6 ± 1.9

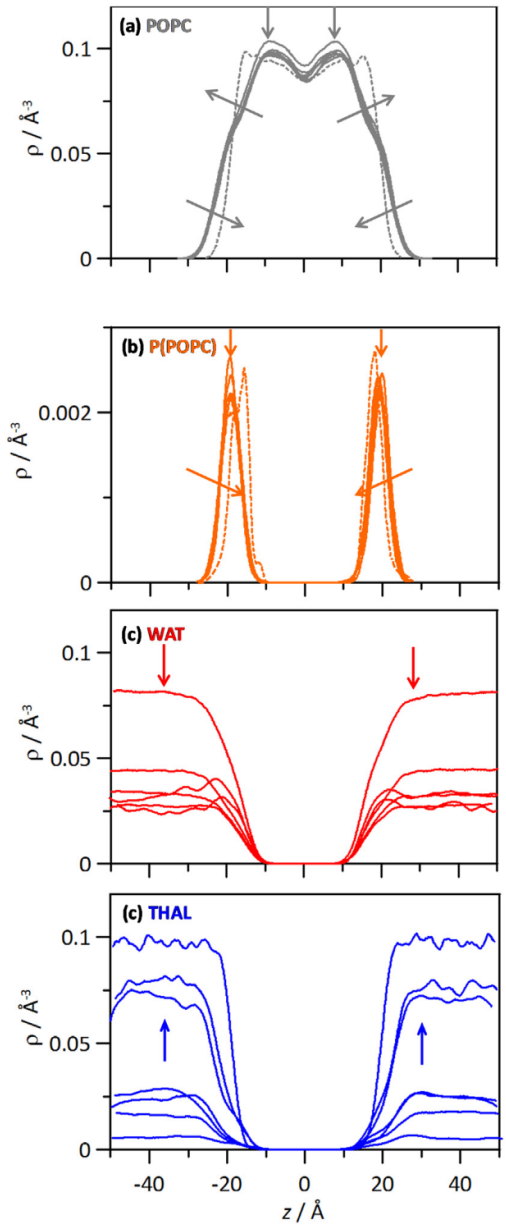

Fig. 2. Number density profiles in the direction perpendicular to POPC-bilayer, z, for THAL + WAT mixtures. Arrows indicate increasing THAL content as in Table 1. Values are obtained for the last 100 ns of the simulations.

calculated using Lorentz-Berthelot mixing rules. The electrostatic interactions were handled with the Particle mesh Ewald method [35].

Simulations were done in the NPT ensemble at 303 K and 1 bar. Langevin thermostat [36], 0.1 ps^{-1} damping constant, was used combined with Berendsen barostat [37], 0.4 ps relaxation time. This combination of Langevin thermostat plus Berendsen barostat has been previously applied with success for MD simulations of lipid bilayers [38]. Although some questions have been raised in the literature about the use of Berendsen barostat for modelling lipid bilayers [39], it has been probed its reliability for the prediction of bilayer properties [40], at a moderate computational cost, and thus being used for simulations of lipid membranes [40–42]. Periodic boundary conditions were considered in the three space directions. MD simulations totalling 1 μs were carried out considering 1 fs time step. Data analysis was carried out with the Membrane Analysis Tool (MEMBPLUGIN) [43] in VMD software.

3. Results and discussion

3.1. Lipid bilayer structural parameters

The present work aims to study the properties of POPC lipid membrane in contact with THAL–water liquid mixtures in the full concentration range even considering pure THAL as reference state, Table 1. MD simulations were carried out for 1 μs total time, which assures a proper characterization of the possible bilayer changes upon interaction with solutions containing THAL. The possible bilayer changes are quantified

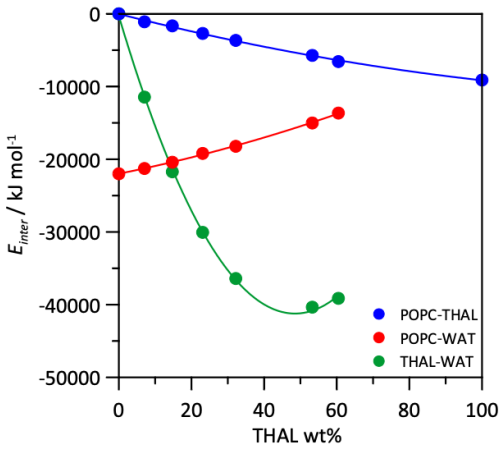

Fig. 3. Intermolecular interaction energy, E_{inter}, for the reported pairs for THAL + WAT mixtures in contact with POPC bilayer function of THAL content (Table 1). Values are obtained for the last 100 ns of the simulations. Errors for E_{inter} (standard deviations) are smaller than the symbols.

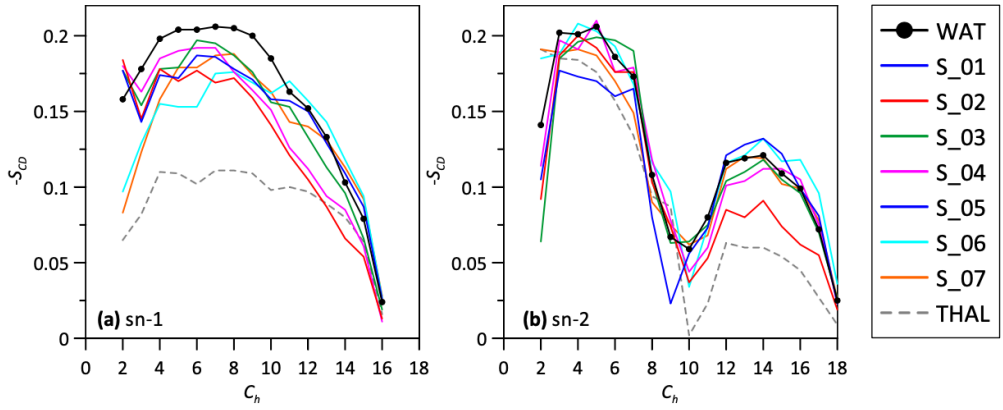

Fig. 4. Order parameter, $-S_{CD}$, for (a) sn-1 (palmitoyl) and (b) sn-2 (oleoyl) tails for THAL + WAT mixtures as a function of THAL content (Table 1). Values are obtained for the last 100 ns of the simulations.

through relevant parameters as reported in Table 2. First, the area per lipid, A_{POPC}, is reported, whose values for POPC bilayer in absence of THAL molecules agrees with literature data both from simulation (0.631 [44] or 0.647 nm^2 [45]) or from experiments (0.643 nm^2 [46]). The presence of THAL molecules leads to the increase of A_{POPC}, i.e. a bilayer expansion effect, although this is a very minor effect given that 6.8% increase is inferred on going from pure water to pure THAL in contact with the membrane corresponding to an increase of 4.4 Å^2. Likewise, this effect of A_{POPC} is present even for low THAL content and does not show a trend with increasing THAL content remaining almost constant in the whole investigated range of THAL concentration. This minor expansion effect due to THAL presence also leads to a decrease in bilayer thickness, h, which is reduced by 10.4% when moving from pure water (with values in suitable agreement with literature [46]) to pure THAL. Therefore, the presence of THAL at the POPC bilayer surface leads to bilayer lateral expansion which produces a decrease in bilayer thickness even if these effects are already present at low THAL concentration and show minor changes when increasing THAL content. The expansive effect has been reported in the literature for POPC bilayers [47] as well as for other lipids such as DPPC [19] or DMPC [48], and it may be justified considering a certain degree of intercalation of THAL molecules between the lipid headgroups, thus increasing lipid to lipid separation in the bilayer. These changes in POPC bilayer properties by THAL are confirmed by results for the width of interdigitation region, ω_p, which remarkably increases upon THAL interaction. Likewise, the vectors defining position of the main POPC groups (θ) show PN (vector joining P from phosphate and N from choline) increasing with THAL content, i.e. POPC groups slightly bend although in a remarkable way only at large THAL content. Likewise, vectors for palmitoyl and oleoyl chains decrease, which means a slight rotation for POPC in the presence of THAL. The changes in POPC orientation agrees with the insertion of THAL molecules close to the lipid headgroups and confirms that the presence of THAL molecules at the bilayer surface leads to changes in structural properties, but the most relevant features of the membranes as their structural integrity upon dehydration are maintained.

3.2. Lipids diffusion

The most relevant change in POPC bilayers upon THAL surface adsorption stands on the lipid lateral diffusion as inferred from self-diffusion coefficients in the xy plane, D_{xy}, which show a large non-linear decrease when increasing THAL content, Table 2. Diffusion coefficients were calculated from the mean-square displacement, msd, of the center of mass of the molecules. The fully diffusive regime was attained during the simulations (1 μs long), which was assured through log-log plots of msd vs simulation time showing unity slope. In the literature the decrease in lateral mobility of phospholipid by interaction with sugars has been confirmed both experimentally and through simulations [49,50]. The decrease in lateral mobility by THAL can be justified considering two main features: *i*) the insertion of THAL molecules in the vicinity of lipid head groups should decrease lateral mobility of these headgroups due to their strong intermolecular forces with the bulky THAL molecules and *ii*) the remarkable increase of lipid interdigitation as reported in Table 2, which leads to increasing tail to tail interactions. Therefore, THAL molecules would lead to bilayer structuring with similar properties close to those in contact with water, which are then maintained upon dehydration, i.e. bilayer vitrification to preserve bilayer structural integrity even in the case of fully dehydrated systems. Further detailed analysis of bilayer properties upon THAL adsorption are discussed in the following section considering the most relevant features.

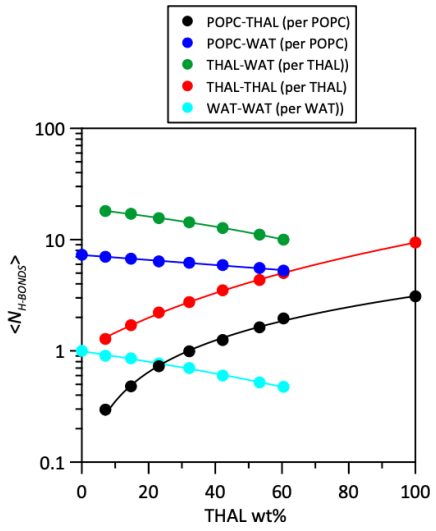

Fig. 5. Average number of hydrogen bonds per molecule, $\langle N_{H\text{-}BONDS} \rangle$, tails for THAL + WAT mixtures as a function of THAL content (Table 1). Values are obtained for the last 100 ns of the simulations.

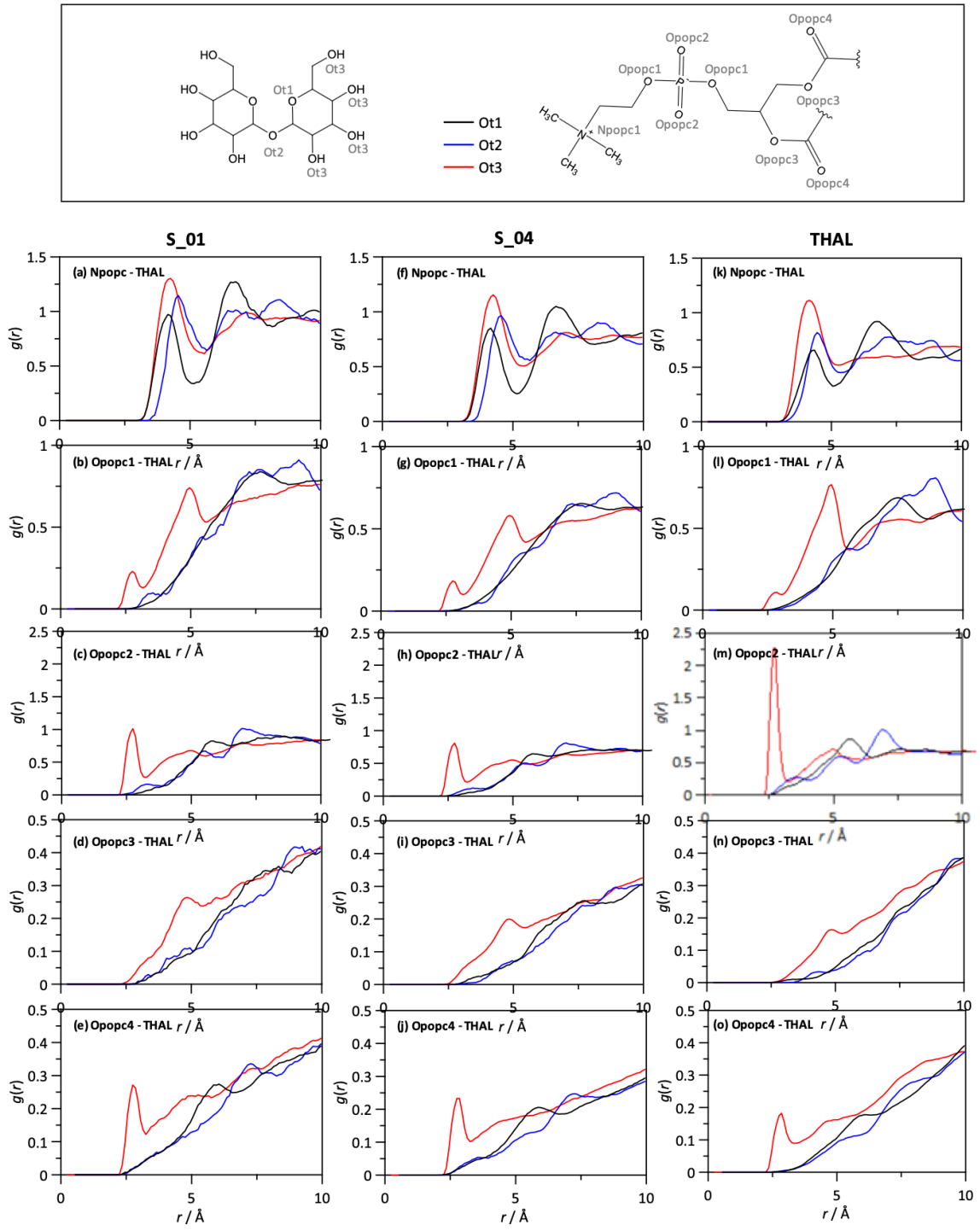

Fig. 6. Site-site radial distribution functions for the reported pairs for THAL + WAT mixtures as a function of THAL content (Table 1). Values are obtained for the last 100 ns of the simulations.

3.3. Lipid adsorption at the interface

The adsorption of THAL molecules at POPC bilayer surfaces is confirmed by the number density profiles reported in Fig. 2. In particular, the number density profiles for POPC molecules, Fig. 2a, show minor changes in POPC distribution upon increasing THAL concentration, whereas a large disruption is reached only with pure THAL. Nevertheless, POPC density profiles are slightly widened when THAL content increases, which agrees with the slight increase in the A_{POPC} reported in Table 2. Likewise, the density profiles for P atoms in phosphate groups reported in Fig. 2b show that bilayer thickness does not change for the position of the maxima; only peaks intensity decrease while widening,

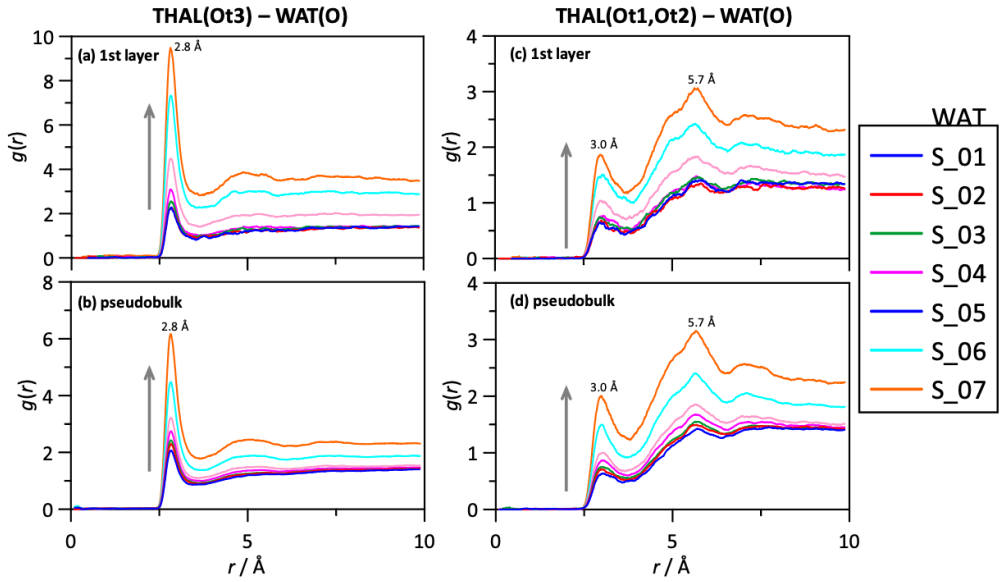

Fig. 7. Site-site radial distribution functions (showing THAL–WAT relevant interactions) for the reported pairs for THAL + WAT mixtures as a function of THAL content (Table 1). Values are obtained for the last 100 ns of the simulations. Values are reported for the layer immediately above the POPC bilayer (1 nm width, 1st layer) and for the region above this 1st layer (pseudobulk). Atom labelling as in Fig. 6. Arrows indicate increase THAL content. Numbers inside each panel indicate the position of relevant peak maxima.

thus agreeing with bilayer lateral expansion when THAL content increases. Regarding the behaviour of the solvent, the density profiles for water and THAL reported in Fig. 2c and d respectively, show water replacement at the bilayer surface by increasing THAL content. THAL molecules remains in surface regions previously occupied by water molecules and remain close to lipid headgroups, phosphate and choline; an increasing amount of adsorbed THAL molecules results when THAL concentration in the solution contacting the bilayer increases. Thus, THAL adsorption in regions close to the lipid headgroups accompanied by minor changes in bilayer properties, mainly increase in lipid interdigitation and slight lipid rotation, and bilayer vitrification are the most relevant features inferred from results in Table 2 and Fig. 2.

The insertion of THAL molecules in the region close to lipid headgroups shows large affinities between THAL and these lipid molecular features as quantified in Fig. 3 by the values of intermolecular interaction energy, E_{inter}. Actually, the comparison of E_{inter} for THAL–POPC vs water–POPC interactions show larger values for water, but this is justified considering the size of water and THAL molecules: the smaller volume of water molecules allows a larger number of interactions with POPC headgroups, whereas the bulkiest character of THAL molecules hinders the development of large number of interactions per POPC molecule. Nevertheless, results in Fig. 3 show decreasing water–POPC E_{inter} in parallel with increasing THAL–POPC E_{inter}, which agrees with the water replacement as reported in Fig. 2c and d. Likewise, results in

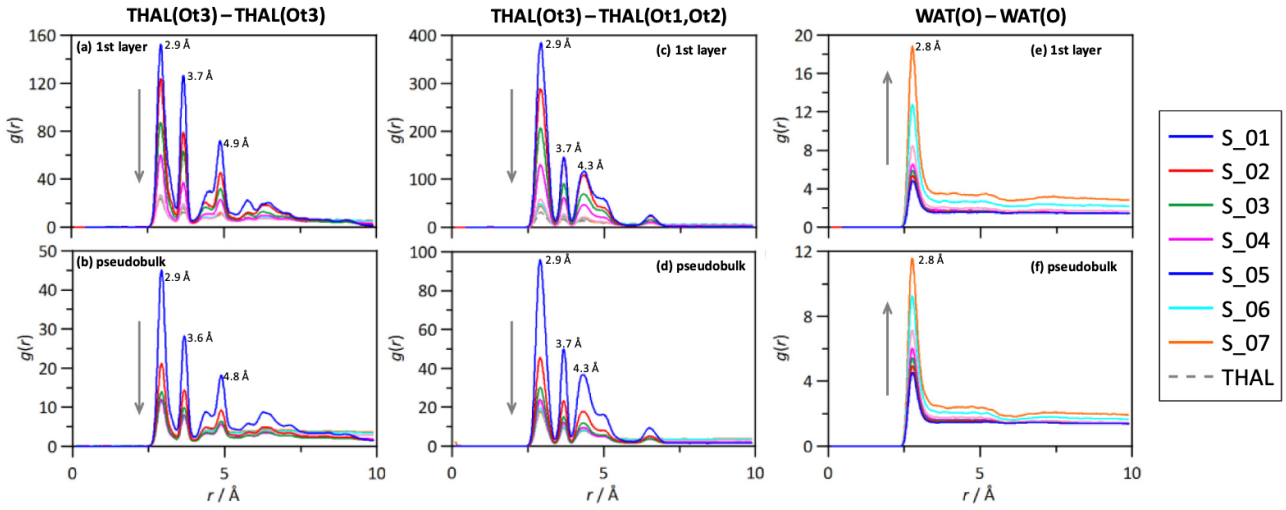

Fig. 8. Site-site radial distribution functions (showing (a to d) THAL–THAL and (e, f) WAT–WAT relevant interactions) for the reported pairs for THAL + WAT mixtures as a function of THAL content (Table 1). Values are obtained for the last 100 ns of the simulations. Values are reported for the layer immediately above the POPC bilayer (1 nm width, 1st layer) and for the region above this 1st layer (pseudobulk). Atom labelling as in Fig. 6. Arrows indicate increase THAL content. Numbers inside each panel indicate the position of relevant peak maxima.

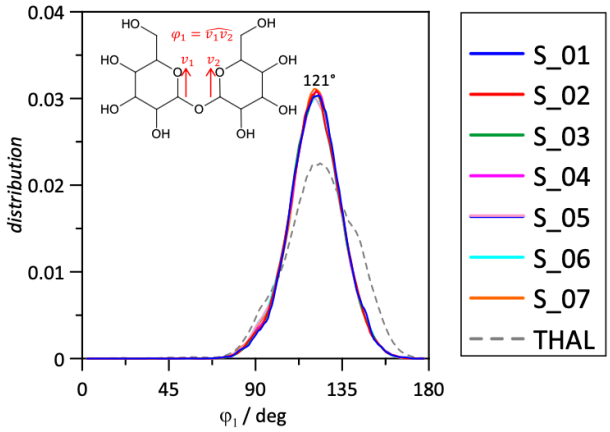

Fig. 9. Intramolecular angular distribution function for the reported vectors, v_1 and v_2, for THAL + WAT mixtures as a function of THAL content (Table 1). Values are obtained for the last 100 ns of the simulations.

Fig. 3 show that water and THAL molecule develop very efficient interactions between them, as confirmed by large E_{inter}, which show that for THAL–water mixtures an additional bilayer stabilization effect appears from the properties of the water/THAL at the bilayer surface.

Results in Fig. 4 show deuterium order parameters, S_{CD}, for sn-1 (palmitoyl) and sn-2 (oleoyl) POPC chains, for POPC bilayer with THAL content. These S_{CD} parameters decrease with addition of THAL both for palmitoyl and oleoyl chains, with large changes for neat THAL in contact with the bilayer, especially for sn-1. As a consequence, a slight disordering effect results due to the presence of THAL, as previously reported in the literature [47]. This effect of THAL on S_{CD} is present even for low THAL content and may be related with the insertion of THAL molecules on the lipid headgroups upon THAL adsorption, which leads to changes for lipid-lipid interactions thus decreasing bilayer ordering. Nevertheless, although bilayer is changed with increasing THAL content, the most relevant features are maintained for all the atoms in palmitoyl and oleoyl chains, and thus the water replacement by THAL maintains bilayer structural integrity. The affinity of THAL for POPC molecules, which leads to surface adsorption without disruption of bilayer structural features, indicates that strong and effective THAL–POPC intermolecular forces are developed. Considering the presence in THAL molecules of hydrogen donor (–OH) and acceptor (—O— and –OH) groups as well as the presence of N and O sites in POPC, hydrogen bonding between THAL and POPC is possible. To this aim, POPC–THAL interaction was quantified and reported in Fig. 5 as well as other relevant hydrogen bonding interactions. Hydrogen bonds were defined with a geometrical criterion considering 3.5 Å and 60° as limit for donor-acceptor sites separation and angle, respectively. The formation of POPC–THAL hydrogen bonds is confirmed in Fig. 5, increasing with THAL content in a non-linear way. The non-linear evolution of hydrogen bonds, especially for POPC–THAL interactions involves two different composition regions separated by THAL 35 wt% content, which agrees with the behaviour of lipid bilayer self-diffusion coefficients reported in Table 2 for which two different linear regions separated by THAL 35 wt% content are also inferred. Therefore, this THAL 35 wt% content may be considered as a critical value separating two very different behaviours in the replacement of water at the bilayer interface by THAL molecules. Likewise, the steric hindrance due to THAL size is confirmed in Fig. 5, where it is confirmed that more than one THAL molecule is hydrogen bonded per molecule only at high THAL concentration. The values for THAL-THAL hydrogen bonds show that THAL molecules are also self-hydrogen bonded upon adsorption at the bilayer surface, thus contributing to the stabilization of the adsorbed layer in spite of the bulkiest character of THAL in comparison with water molecules. Likewise, results in Fig. 5 show that the number of POPC–THAL hydrogen bonds are lower than THAL–THAL ones, which indicates a competing effect for the hydrogen bonding sites. Therefore, the POPC molecules compete with THAL for hydrogen bonding but the large trend of THAL molecules to be self-hydrogen bonded maintains these interactions even after THAL adsorption at the bilayer surface, and thus, this minor disruption of THAL intermolecular forces accompanied by the simultaneous interaction with the POPC molecules contributes to the stabilization of the bilayer as well of the solution in contact with it. The water–POPC hydrogen bonding is largely maintained even for high THAL content, which shows that, in spite of the water molecules replaced by THAL molecules as reported in Fig. 2c and d, a remarkable amount of water remains in the vicinity of lipid headgroups being hydrogen bonded in parallel to the adsorption of THAL. This effect can be justified considering that the bulkiest character of THAL molecules leaves empty spaces on the bilayer surface which can be occupied by water molecules occupying additional hydrogen bonding sites in POPC molecules, thus leading to very effective hydrogen bonding of POPC molecules with both POPC and water molecules. These gradual changes in bilayer hydrogen bonding upon dehydration by water replacement are on the roots of the stabilization of the bilayer for large THAL content. Additionally, water and THAL are able to develop effective hydrogen bonding as shown in Fig. 5, which the adsorbed layers on the surface are characterized by large hydrogen bonding among all the molecular features, thus leading to highly stable structures and minor disruption of bilayer.

3.4. Structuring of adsorbed layers

The structuring of the bilayer–liquid phase interfaces, with attention to POPC–THAL interactions, are analysed in detail by using radial distribution functions, RDFs, for relevant molecular sites. Results in Fig. 6 show RDFs for the interaction between —O— and –OH sites of THAL and N or O sites in POPC molecules at different THAL concentrations. The reported results show preferential interaction of THAL molecules with N sites (choline group) in POPC, Fig. 6a, f and k show peaks for N–THAL interactions at roughly 4.0 Å followed by a second peak at 7.0 Å, which are present in the whole concentration range. These peaks are present both for THAL —O— sites, Ot1 and Ot2 sites corresponding to O in rings and O joining hexose rings, as well as for THAL hydroxyl sites. These N-POPC related RDFs are in contrast with the remaining panels in Fig. 6 corresponding to the interaction with O-POPC sites both for phosphate groups and head sites at palmitoyl and oleoyl chains, which show only very minor features. Therefore, hydrogen bonding as reported in Fig. 5 would correspond to interactions with choline group and in very minor extension with remaining O– sites. Thus, insertion of THAL molecules is carried out in the vicinity of the POPC choline group, which leaves the remaining POPC sites accessible to water molecules. This would justify the extension of water–POPC hydrogen bonding as reported in Fig. 5. The simultaneous presence of THAL and water molecules at the bilayer surface allows THAL–water hydrogen bonding, Fig. 5, thus THAL–water RDFs are reported in Fig. 6. The THAL–water interactions are mainly developed through THAL hydroxyl sites in hexose rings, Fig. 7a, whereas interaction through THAL —O— sites are produced in minor extension, Fig. 7c. The behaviour of THAL–water interactions at the bilayer surface, Fig. 7a and c, is analogous to that in bulk liquid phase, Fig. 7b and d, thus the properties of THAL solution are maintained upon adsorption at the interface without large disruption of the intermolecular forces. Likewise, THAL–THAL and water–water interactions are maintained upon adsorption on the surface, Fig. 8, with the corresponding RDF peaks maintained as in the bulk liquid phase. Additionally, RDFs in Fig. 8a show confirm THAL–THAL hydrogen bonding, Fig. 5. The adsorption of THAL in the vicinity of POPC choline sites allows the insertion of water molecules in the same POPC molecules and maintaining water–THAL, water–water and THAL–THAL interactions as in the liquid phase as well as maintaining the structuring of the bilayer. Therefore, the interaction with the POPC

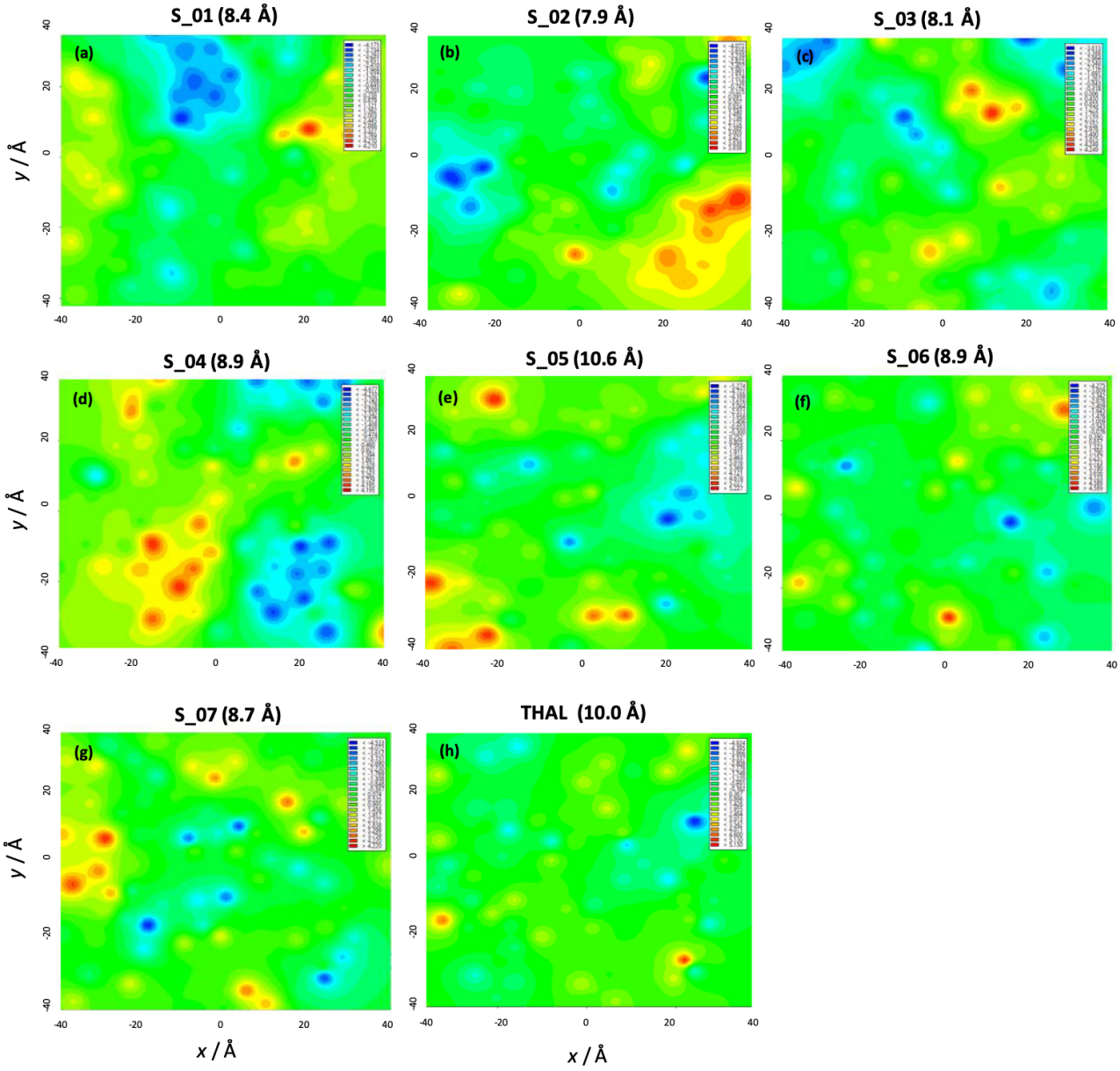

Fig. 10. Leaflet deformation maps, showing the difference with the average thickness (h in Table 1), for THAL + WAT mixtures as a function of THAL content (Table 1). Values are obtained for the last 100 ns of the simulations. Parenthesized values show the deformation range.

bilayer is accompanied by minor disruption of solutions structuring accompanied by stabilization of bilayer structuring for wide range of THAL content, including neat THAL. The adsorption of THAL molecules should lead to structural changes upon interaction with the bilayer, the planarity of the molecule is studied through the relative orientation of the vectors for the two hexose rings as reported in Fig. 9. These results show that adsorbed THAL molecules are largely non-planar with both hexose rings adopting a configuration at 121°, i.e. skewed hexose rings. This configuration is also present in THAL–water mixtures in absence of lipid membranes [51] with the angle being 104°, and thus skewing is increased upon adsorption at the bilayer surface. Nevertheless, the most relevant THAL structural features are maintained at the bilayer surface, which would justify the negligible changes reported in Figs. 7 and 8, as well as the hydrogen bonding for THAL-water solutions after adsorption at the bilayer surface.

The literature results have showed bilayer buckling and THAL preference for highly curved regions of bilayer surfaces for improving lipid-THAL interactions [52]. Surface curvature effect are difficult to consider from MD simulations because of the limited size of the applied bilayer models. Nevertheless, irregularities in bilayer thickness are studied in this work through leaflet deformation maps, which show deviations with average thickness (Table 2). Blue spots in Fig. 10 show regions with lower thickness than average, i.e. bilayer contraction, and red spots correspond to thickness larger than average, i.e. bilayer expansion. These results in Fig. 10 show highly irregular distribution of bilayer thicknesses, especially for low to moderate THAL content whereas for THAL rich mixtures, including even the pure THAL case, the thickness distribution results to be more homogeneous. These results point to curved surfaces for low THAL content with an increase of planarity with increasing THAL concentration, i.e. dehydration. This behaviour

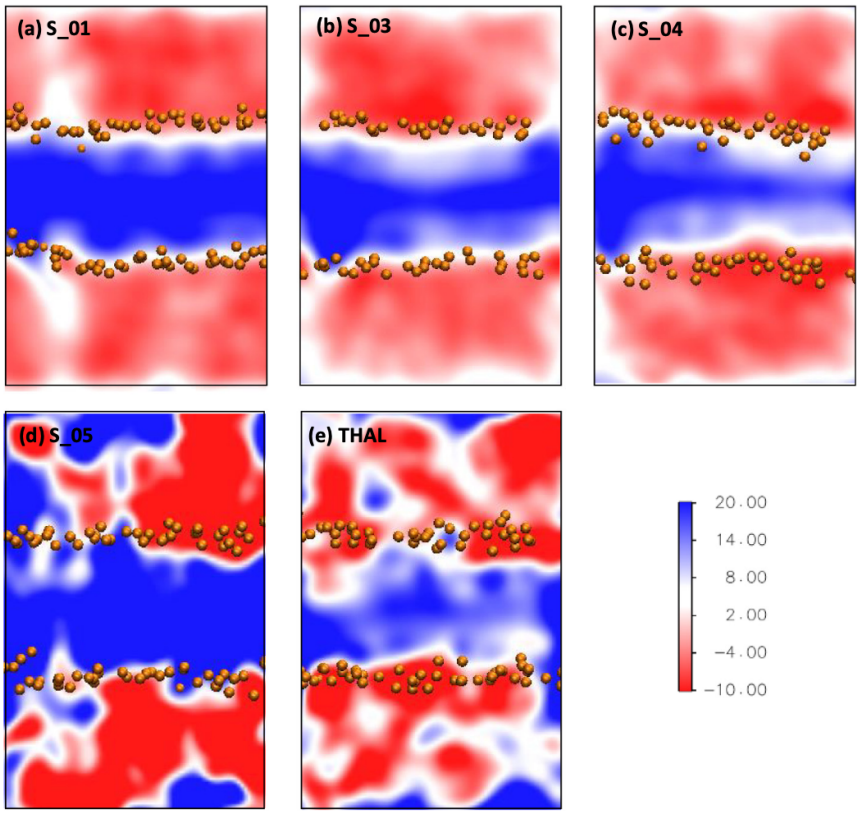

Fig. 11. Electrostatic potential along perpendicular direction to POPC bilayer surface for THAL + WAT mixtures as a function of THAL content (Table 1). Values are obtained for the last 100 ns of the simulations. Orange spheres show the position of P atoms in POPC molecules.

may be justified considering the preference of THAL molecules for curved regions. Curved interfaces would be present for water rich mixtures. For THAL rich solutions, the surface is homogeneously covered by THAL molecules, and thus the preference for curved regions vanishes because of strong THAL -THAL interactions as well as the presence of at least one THAL molecule per (choline) POPC site.

3.5. Electrostatic properties of lipid bilayers

The electrostatic properties of POPC bilayer may be changed upon dehydration with increasing THAL content. To this aim, the electrostatic potential in the direction perpendicular to the bilayer surface is reported in Fig. 11 for the full THAL concentration range. The presence of increasing THAL content in the surface changes electrostatic properties of the membrane, this effect being noted especially relevant for high THAL content. Likewise, the properties of lipid tails regions, i.e. bilayer centre, are also affected by the presence of adsorbed THAL molecules. The presence of largely polar THAL molecules induces charge accumulation at the interface, which also effects the charge distribution in the hydrophobic regions of the bilayers. Therefore, although THAL adsorption does not change most of the structural properties of the POPC bilayer, their electrostatic properties are changed. Dehydration with increasing THAL content leads to membrane vitrification as well as leading to more charged bilayers.

4. Conclusions

The properties of POPC lipid bilayers in contact with THAL + solutions are studied by using molecular dynamics simulations as a function of increasing THAL content to mimic membranes dehydration process. THAL molecules are adsorbed on the bilayer surface interacting mainly with choline POPC groups, thus developing hydrogen bonds with lipid molecules. Nevertheless, the bulkiest characteristic of THAL molecules leaves free sites in POPC molecules, thus facilitating water molecules to interact with lipid layers and maintaining water content at the surface even for high THAL content. THAL molecules also develop hydrogen bonding between them as well as with water molecules, thus leading to a highly structured layer on the bilayer surface with properties similar to those of THAL + water mixtures in absence of the membrane. The increasing THAL content upon dehydration leads to minor changes in bilayer structural properties, with slight bending of POPC molecules, minor expansion on the bilayer plane, and increase of interdigitation. The main changes upon THAL adsorption stand on the decrease of lipids lateral mobility, which leads to a glassy state maintaining the structural features but also changing the electrostatic properties of the bilayer. THAL molecules are able to maintain bilayer structuring upon dehydration, where water molecules are present at the interface with THAL molecules interacting with very specific lipid sites even for high THAL content. Thus, the water replacement mechanism is only partially fulfilled considering that both water and THAL molecules coexist at the interface for large concentration ranges, with both molecules collaborating for the stabilization of the bilayers upon dehydration.

Acknowledgements

This work was funded by the European Union's Horizon 2020 program under the Marie Skłodowska-Curie "Research and Innovation Staff Exchange (RISE)" (DRYNET; Grant No. 734434). The statements made herein are solely the responsibility of the authors.

References

[1] J.S. Clegg, Cryptobiosis—a peculiar state of biological organization, Comp. Biochem. Physiol. 128B (2001) 613–624.
[2] J.H. Crowe, F.A. Hoekstra, L.M. Crowe, Anhydrobiosis, Annu. Rev. Physiol. 54 (1992) 579–599.
[3] G.D. Elliott, S. Wang, B.J. Fuller, Cryoprotectants: a review of the actions and applications of cryoprotective solutes that modulate cell recovery from ultra-low temperatures, Cryobiology 76 (2017) 74–91.
[4] L.M. Crowe, Lessons from nature: the role of sugars in anhydrobiosis, Comp. Biochem. Physiol. 131A (2002) 505–513.
[5] J.H. Crowe, Trehalose as a "chemical chaperone": fact and fantas, in: P. Csermely, L. Vigh (Eds.), Molecular Aspects of the Stress Response: Chaperones, Membranes and Network, 13, Landes Bioscience and Springer Science + Business Media 2007, pp. 497–503.
[6] K.A. Morano, Anhydrobiosis: drying out with sugar, Curr. Biol. 24 (2014) R1121–R1123.
[7] N.K. Jain, I. Roy, Effect of trehalose on protein structure, Protein Sci. 18 (2009) 24–36.
[8] J.H. Crowe, L.M. Crowe, D. Chapman, Preservation of membranes in anhydrobiotic organisms: the role of trehalose, Science 223 (1984) 701–703.
[9] A.E. Oliver, E.L. Kendall, M.C. Howland, B. Sanii, A.P. Shreve, A.N. Parikh, Protecting, patterning, and scaffolding supported lipid membranes using carbohydrate glasses, Lab Chip 8 (2008) 892–897.
[10] Y. Wang, S. Quang, H. Ma, D. Liu, F. Xie, G. Chen, B. Wang, M. An, F.A. Ding, Review on the protection mechanism of trehalose on plant tissues and animal cells, Agric. Biotechnol. 8 (2019) 29–34.
[11] L.M. Crowe, J.H. Crowe, A. Rudolph, C. Womersley, L. Appel, Preservation of freeze-dried liposomes by trehalose, Arch. Biochem. Biophys. 242 (1985) 240–247.
[12] S. Ohtake, C. Schebor, J.J. de Pablo, Effects of trehalose on the phase behavior of DPPC–cholesterol unilamellar vesicles, Biochim. Biophys. Acta 1758 (2006) 65–73.
[13] J.S. Clegg, P. Seitz, W. Seitz, C.F. Hazlewood, Cellular responses to extreme water loss: the water replacement hypothesis, Cryobiology 19 (1982) 306–316.
[14] E.A. Golovina, A.V. Golovin, F.A. Hoekstra, R. Faller, Water replacement hypothesis in atomic detail—factors determining the structure of dehydrated bilayer stacks, Biophys. J. 97 (2009) 490–499.
[15] J. Wolfe, G. Bryant, Freezing, drying, and/or vitrification of membrane-solute-water systems, Cryobiology 39 (1999) 103–129.
[16] B.A.C. Horta, L. Peric-Hassler, P.H. Hünenberger, Interaction of the disaccharides trehalose and gentiobiose with lipid bilayers: a comparative molecular dynamics study, J. Mol. Graph. Model. 29 (2010) 331–346.
[17] B. Kent, T. Hunt, T.A. Darwish, T. Hauß, C.J. Garvey, G. Bryant, Localization of trehalose in partially hydrated DOPC bilayers: insights into cryoprotective mechanisms, J. R. Soc. Interface 11 (2014), 20140069. .
[18] M.A. Villareal, S.B. Díaz, E.A. Disalvo, G.G. Montich, Molecular dynamics simulation study of the interaction of trehalose with lipid membranes, Langmuir 20 (2004) 7844–7851.
[19] C.S. Pereira, R.D. Lins, I.C. Handrasekhar, L.C.G. Freitas, P.H. Hünenberger, Interaction of the disaccharide trehalose with a phospholipid bilayer: A molecular dynamics study, Biophys. J. 86 (2004) 2273–2285.
[20] A. A. Skibinsky, R.M. Venable, R.W. Pastor, A molecular dynamics study of the response of lipid bilayers and monolayers to trehalose, Biophys. J. 89 (2005) 4111–4121.
[21] J. Kapla, O. Engström, B. Stevensson, J. Wohlert, G. Widmalm, A. Maliniak, Molecular dynamics simulations and NMR spectroscopy studies of trehalose–lipid bilayer systems, Phys. Chem. Chem. Phys. 17 (2015) 22438–22447.
[22] J. Liu, C. Chen, C. Lu, W. Li, Different mechanisms on the stabilization of POPC membrane by trehalose upon varied mechanical stress, J. Mol. Liq. 275 (2019) 839–848.
[23] H.D. Andersen, C. Wang, L. Arlethh, G.H. Peters, P. Westh, Reconciliation of opposing views on membrane–sugar interactions, PNAS 108 (2011) 1874–1878.
[24] J.H. Crowe, Anhydrobiosis: an unsolved problem, Plant Cell Environ. 37 (2014) 1491–1493.
[25] M.J. Harvey, G. Giupponi, G. De Fabritis, ACEMD: accelerating biomolecular dynamics in the microsecond time scale, J. Chem. Theory Comput. 5 (2009) 2371–2377.
[26] G. Van Meer, D.R. Voelker, G.W. Feigenson, Membrane lipids: where they are and how they behave, Nat. Rev. Mol. Cell Biol. 9 (2008) 112–124.
[27] J. Liu, C. Chen, W. Li, The influence of water and trehalose content on the stabilization of POPC membrane upon rapid heating studied by molecular simulations, Fluid Phase Equilibr 474 (2018) 27–109.
[28] E.L. Wu, X. Cheng, S. Jo, H. Rui, K.C. Song, E.M. Dávila-Contreras, Y. Qi, J. Lee, V. Monje-Galvan, R.M. Venable, J.B. Kaluda, W. Im, Charmm-GUI membrane builder toward realistic biological membrane simulations, J. Comput. Chem. 35 (2014) 1997–2004.
[29] L. Martínez, R. Andrade, E.G. Birgin, J.M. Martínez, PACKMOL: a package for building initial configurations for molecular dynamics simulations, J. Comput. Chem. 30 (2009) 2157–2164.
[30] J.B. Klauda, R.M. Venable, J.A. Freites, J.W. O'Connor, D.J. Tobias, C. Mondragon-Ramirez, I. Vorobyov, A.D. MacKerell Jr., R.W. Pastor, Update of the CHARMM all-atom additive force field for lipids: validation on six lipid types, J. Phys. Chem. B 114 (2010) 7830–7843.
[31] R.W. Pastor, A.D. MacKerell, Development of the CHARMM force field for lipids, J. Phys. Chem. Lett. 2 (2011) 1526–1532.
[32] W.L. Jorgensen, J. Chandrasekhar, J.D. Madura, R.W. Impey, M.L. Klein, Comparison of simple potential functions for simulating liquid water, J. Chem. Phys. 79 (1983) 926–935.
[33] S. Boonstra, P.R. Onck, E. van der Giessen, CHARMM TIP3P water model suppresses peptide folding by solvating the unfolded state, J. Phys. Chem. B 120 (2016) 3692–3698.
[34] K. Vanommeslaeghe, E. Hatcher, C. Acharya, S. Kundu, S. Zhong, J. Shim, E. Darian, O. Guvench, P. Lopes, I. Vorobyov, A.D. Mackerell Jr., CHARMM general force field: a force field for drug-like molecules compatible with the CHARMM all-atom additive biological force fields, J. Comput. Chem. 31 (2010) 671–690.
[35] T. Darden, D. York, L. Pedersen, Particle mesh Ewald: An N·log(N) method for Ewald sums in large systems, J. Chem. Phys. 98 (1993) 10089–10092.
[36] J.A. Izaguirre, D.P. Catarello, J.M. Wozniak, R.D. Skeel, Langevin stabilization of molecular dynamics, J. Chem. Phys. 114 (2001) 2090–2098.
[37] H.J.C. Berendsen, J.P.M. Postma, W.F. van Gunsteren, A. DiNola, J.R. Haak, Molecular dynamics with coupling to an external bath, J. Chem. Phys. 81 (1984) 3684–3690.
[38] B.D. Madej, I.R. Gould, R.C. Walker, A parameterization of cholesterol for mixed lipid bilayer simulation within the Amber Lipid14 force field, J. Phys. Chem. B 119 (2015) 12424–12435.
[39] M.R. Shirts, Simple quantitative tests to validate sampling from thermodynamic ensembles, J. Chem. Theor. Comput. 9 (2013) 909–926.
[40] L. Chen, J. Chen, G. Zhou, Y. Wang, C. Xu, X. Wang, Molecular dynamics simulations of the permeation of bisphenol A and pore formation in a lipid membrane, Sci. Rep. 6 (2016) 33399.
[41] N.I. Ercan, P. Stroeve, J.W. Tringe, R. Faller, Molecular dynamics modeling of methylene blue–DOPC lipid bilayer interactions, Langmuir 34 (2018) 4314–4323.
[42] M. Atilhan, L.T. Costa, S. Aparicio, On the behaviour of aqueous solutions of deep eutectic solvents at lipid bilayers, J. Mol. Liq. 247 (2017) 116–125.
[43] R. Guixa-González, I. Rodríguez-Espigares, J.M. Ramírez-Anguita, P. Carrió-Gaspar, H. Martinez-Seara, T. Giorgino, J. Selent, MEMBPLUGIN: studying membrane complexity in VMD, Bioinformatics 30 (2014) 1478–1480.
[44] N. Kucerka, M.P. Nieh, J. Katsaras, Fluid phase lipid areas and bilayer thicknesses of commonly used phosphatidylcholines as a function of temperature, Biochim. Biophys. Acta 1808 (2011) 2761–2771.
[45] J.B. Klauda, R.M. Venable, A. Freites, J.W. O'Connor, D.J. Tobias, C. Mondragon-Ramirez, I. Vorobyov, A.D. MacKerell, R.W. Pastor, Update of the CHARMM all-atom additive force field for lipids: validation on six lipid types, J. Phys. Chem. B 114 (2010) 7830–7843.
[46] G. Shahane, W. Ding, M. Palaiokostas, M. Orsi, Physical properties of model biological lipid bilayers: insights from all-atom molecular dynamics simulations, J. Mol. Model. 25 (2019) 76.
[47] E.A. Golovina, A. Golovin, F.A. Hoekstra, R. Faller, Water replacement hypothesis in atomic details: effect of trehalose on the structure of single dehydrated POPC bilayers, Langmuir 26 (2010) 11118–11126.
[48] J. Kapla, J. Wohlert, B. Stevenson, O. Engström, G. Widmalm, A. Maliniak, Molecular dynamics simulations of membrane–sugar interactions, J. Phys. Chem. B 117 (2013) 6667–6673.
[49] G. van den Bogaart, N. Hermans, V. Krasnikov, A.H. de Vries, B. Poolman, On the decrease in lateral mobility of phospholipids by sugars, Biophys. J. 92 (2007) 1598–1605.
[50] M. Tang, A.J. Waring, M. Hong, Trehalose-protected lipid membranes for determining membrane protein structure and insertion, J. Magn. Reson. 184 (2007) 222–227.
[51] A. Kumar, A. Cincotti, S. Aparicio, A theoretical study on trehalose + water mixtures for dry preservation purposes, Molecules 25 (2020) 1435.
[52] J. Kapla, B. Stevensson, A. Maliniak, Coarse-grained molecular dynamics simulations of membrane–trehalose interactions, J. Phys. Chem. B 120 (2016) 9621–9631.